Supporting information

Structure-activity relationships of LDH catalysts for the glucose-to-fructose isomerisation in ethanol

Krisztina Karádi,[a] Thanh Truc Nguyen,[b] Adél Anna Ádám,[a] Kornélia Baán,[c] András Sápi,[c] Ákos Kukovecz,[c] Zoltán Kónya,[c] Pál Sipos,[d]* István Pálinkó[a]⑤ and Gábor Varga[e]*¥

[a]*Department of Organic Chemistry and Materials and Solution Structure Research Group, University of Szeged, Dóm tér 8, Szeged, H-6720 Hungary*
[b]*Australian Institute for Bioengineering and Nanotechnology, The University of Queensland, Brisbane, QLD 4072, Australia*
[c]*Department of Applied and Environmental Chemistry and Interdisciplinary Excellence Centre, Institute of Chemistry, University of Szeged, Rerrich Béla tér 1, Szeged, H-6720 Hungary*
[d]*Department of Inorganic and Analytical Chemistry and Materials and Solution Structure Research Group, University of Szeged, Dóm tér 7, Szeged, H-6720 Hungary*
[e]*Department of Physical Chemistry and Materials Science and Materials and Solution Structure Research Group, University of Szeged, Rerrich Béla tér 1, Szeged, H-6720 Hungary*

*Corresponding authors: **P. Sipos** (sipos@chem.u-szeged.hu), **G. Varga** (gabor.varga5@chem.u-szeged.hu)
⑤ passed away
¥ Present address: Australian Institute for Bioengineering and Nanotechnology, The University of Queensland, Brisbane, QLD 4072, Australia

S1. EXPERIMENTAL PART

S1.1. Materials

All the AR-grade chemical reagents were purchased from Merck and Sigma-Aldrich and used as received without further purification.

S1.2. Synthesis of ion intercalated hydrotalcites (Mg$_X$Al-L(ayered)D(ouble)H(ydroxides)) and hydrocalumites (Ca$_2$Al-LDH)

Carbonate-containing hydrotalcites were prepared by using a co-precipitation method carried out at constant pH of 10.0. At this pH, based on the literature data, well-crystallized, non-porous, phase pure LDH with hexagonally shaped morphology and medium crystallite size (13–21 nm) can be produced.[1] During the synthesis procedure, two aqueous solutions – marked as **A** and **B** – were used. For solution **A**, the appropriate amount of Mg(NO$_3$)$_2$ × 6H$_2$O (c = 0.06–0.12 M, depending on the Mg-to-Al molar ratio) and Al(NO$_3$)$_3$ × 9H$_2$O (c = 0.03 M) were dissolved in 100 mL distilled water while solution **B** was prepared by dissolving Na$_2$CO$_3$ (c = 0.20 M) and NaOH in 100 mL of distilled water. Then solution **A** was added into solution **B** in one portion. The obtained suspension was stirred constantly for 8 hours at room temperature under N$_2$ atmosphere. The final slurry was filtered, washed three times with distilled water (3×100 mL) and dried at 70°C overnight. The final products were denoted as Mg$_2$Al-LDH, Mg$_3$Al-LDH and Mg$_4$Al-LDH. The preparation of nitrate-containing and chloride-containing hydrotalcites was carried out *via* the same procedure as described above using NaNO$_3$ and NaCl salts instead of Na$_2$CO$_3$ for making up solution **B**. The final products thus produced were marked as NO$_3$–Mg$_X$Al-LDH and Cl–Mg$_X$Al-LDH (X = 2, 3, 4).

The synthesis of hydrocalumites followed almost the same method as above, except for setting a pH of 13.1 at which co-precipitation is possible.[2] It is noteworthy that phase-pure carbonate-containing hydrocalumite cannot be prepared by the co-precipitation method because the by-product CaCO$_3$ is precipitated, which is preferred to the formation of LDH under the reaction conditions presented. Therefore, nitrate- and chloride-containing hydrocalumites prepared in this way and named NO$_3$–Ca$_2$Al-LDH and Cl–Ca$_2$Al-LDH, respectively. It should be noted that there was no possibility to change the ratio of Ca-to-Al in the hydrocalumites, as this ratio is fixed due to structural requirements.

For comparison, hydrotalcite with a nominal Mg-to-Al ratio of 3:1 was synthesized according to the method of Fukuoka *et al.*[3] The catalyst thus prepared proved to be the most efficient LDH-based catalyst in alcoholic solvents to date. Briefly, 50 mL of Mg(NO$_3$)$_2$ × 6H$_2$O-

(0.09 M) and $Al(NO_3)_3 \times 9H_2O$-containing (0.03 M) aqueous solution was prepared and added dropwise from a syringe to distilled water of 25 mL, simultaneously with 50 mL of aqueous solution containing $(NH_4)_2CO_3$ (0.30 M). Then an appropriate amount of 30.0 wt% NH_3 solution was added to the obtained suspension to adjust a pH of 7.6–8.0, which was monitored with a pH sensitive glass electrode. The suspension was then stirred vigorously at 65°C for 3 hours. The slurry obtained was filtered, washed with distilled water (500 mL) and dried at 100°C for 18 hours. The white solid obtained was designated F-Mg_3Al-LDH (F as in Fukuoka).

S1.3. Preparation of dehydrated, calcined and calcined-rehydrated hydrotalcites/hydrocalumites

To determine the effects of surface hydration on the catalytic performance of LDHs, a partial dehydration/calcination process was introduced. In this process, the LDHs thus prepared were heat treated for 8 hours at different temperatures in the order 135, 200, 330 and 500°C. In the case of the hydrocalumites, the application of a N_2 atmosphere was necessary to avoid the formation of $CaCO_3$ as a by-product. Taking advantage of the well-known memory effect of LDHs, the fully dehydrated/calcined (T = 500°C) samples were rehydrated.[3] For this purpose, a portion of 0.3 g of calcined LDH was added to 50 mL of aqueous solution of $NaNO_3$ (0.30 M) and this suspension was then stirred vigorously for 24 hours at 60°C under a nitrogen atmosphere. The slurry obtained was filtered, washed with decarbonated water (3 × 60 mL) and dried overnight at 80°C. Decarbonated water was used during the rehydration process. The dehydration/rehydration process was also used to produce carbonate-containing hydrocalumite. For this purpose, a Na_2CO_3 solution was used during rehydration instead of a solution containing $NaNO_3$.

S1.4. Tuning the morphology/crystallite size of LDHs by introducing post-synthetic treatments

Post-synthetic treatments were used to alter the crystallite size and morphology of LDHs, which was likely to be one of the key parameters for improving the catalytic performance of LDHs. In order to decrease the crystallite size of Mg_2Al-LDH, hydrothermal treatment was carried out according to the procedure presented by Xu *et al.*[4] Briefly, a 1.50 g portion of Mg_2Al-LDH was suspended in 40 mL of distilled water and the suspension was poured into a PTFE-lined stainless steel autoclave of 50 mL. The autoclave was then placed in a preheated oven and hydrothermal treatment was carried out at 100°C for 16 hours. After air cooling, the suspension was centrifuged, washed twice with distilled water and dried at 70°C overnight.

To achieve a larger crystallite size of Mg_2Al-LDH compared to the starting material, a hot ageing treatment was carried out according to the procedure of Duan et al.[5] For this purpose, the co-precipitation method described above should necessarily be modified. Specifically, after stirring, the resulting mixture was aged at 100°C for 13 hours, then the slurry obtained was filtered, washed several times with distilled water and dried at 100°C for 24 hours.

S1.5. Characterization methods

XRD patterns were taken with a Rigaku XRD MiniFlex II instrument using CuKα radiation (λ = 0.15418 nm) and an accelerating voltage of 40 kV at 30 mA. The characteristic reflections were identified based on the database JCPDS-ICDD (Joint Committee of Powder Diffraction Standards- International Centre for Diffraction Data). The distance of one layer together with the interlayer distance was calculated by Bragg's law:

$$n\lambda = 2d_{hkl}\sin\theta \qquad\qquad \text{S1}$$

where n is an integer; λ is the wavelength of the incident light, d_{hkl} is the lattice spacing and θ is the angle of incidence. Crystallite size were determined by Scherrer equation:

$$D = \frac{K\lambda}{\beta\cos\theta} \qquad\qquad \text{S2}$$

where K is the Scherrer constant, λ is wave length of the X-ray beam used, β is the Full width at half maximum (FWHM) of the peak and θ is the Bragg angle.

Zeta potentials were ascertained with a Malvern NanoZSD dynamic light scattering (DLS) device equipped with a 4 mW laser source operating at 633 nm wavelength. For specific surface area study, BET (Brunauer-Emmett-Teller) N_2-sorption experiments were performed, using a NOVA3000 (Quantachrome) instrument. *Prior to* the measurements, the solids were degassed with N_2 at 100°C for 5 hours under vacuum to clean the surface from the adsorbents. The measurements were carried out at the temperature of liquid N_2.

The morphology of the samples prepared were studied by scanning electron microscopy (SEM). The SEM images were acquired on an S-4700 electron microscope (Hitachi) with an accelerating voltage of 10–18 kV. The actual Mg-to-Al ratios of the samples were determined with an Agilent 7900 ICP-MS (inductively coupled plasma–mass spectrometry) (Agilent Technologies) device. For the quantitative analysis, ICP multielement standard solution IV (CertiPUR) was used. *Prior to* the measurements, an accurately measured amount (a few milligrams) of the solids was dissolved in 5 mL of cc. HCl. After dissolution, the samples were diluted to 100 mL with distilled water and filtered.

For the glucose adsorption study, 100 mg of LDH samples were suspended in ethanolic solutions of 14.0 mL containing 250–2500 mg/L glucose at 40°C. The samples were continuously stirred for 2 hours. After completion of the reaction, 1 mL aliquots were filtered with a 0.22 μm membrane filter, and the concentration of glucose in the filtrate was determined by NMR spectroscopy (see below, *S1.6.*). The increase in the hydrodynamic radius of LDH samples due to the glucose adsorption was also followed by dynamic light scattering (DLS) technique using Malvern NanoZSD DLS device for this purpose as well. The cumulative method was applied to fit the correlation functions, which were collected for 20 seconds. Data collection was conducted at 175° scattering angle at 25°C.

The basicity of the samples was characterized by non-aqueous acid-base titrations. For these experiments, 50 mg of the sample were then suspended in a solution mixture of 20 mL ethanol, and 0.5 mL of a 0.2% indicator ethanolic solution containing bromothymol blue (pK_a = 7.1), phenolphthalein (pK_a = 9.3), and indigo carmine (pK_a = 12.2) was also added. Thereafter, the solution was titrated against benzoic acid (0.01 M), while stirring continuously at 500 rpm.[6]

CO_2-temperature programmed desorption (TPD) measurements could provide more accurate results of intrinsic basicity. Unfortunately, for practical reasons, this method cannot be used for the study of carbonate-containing hydrated hydrotalcites.[7] However, in order to validate our results obtained by acid-base titration, the basic sites of the calcined samples were also characterized by the CO_2-TPD technique, where there are no limitations in the absence of water- and charge-compensating anions. TPD Measurements were performed using a Hewlett-Packard 5890 GC system equipped with a TCD detector. Prior to measurements, a quartz tube was loaded with a portion of the sample (100 mg) followed by the first purge in a flow of He (50 mL/min) at room temperature for 10 min to remove impurities. The temperature was then raised to 450°C at a ramp rate of 10°C/min and then held for 1 hour to remove water and other impurities. The temperature was then lowered to 100°C. Finally, the gas was changed to CO_2 in He (30 mL/min CO_2, 50 mL/min He) and circulated over the sample for 1 h.

S1.6. Catalytic isomerization of glucose to fructose

The previously described composites were tested as catalysts for the isomerization reaction. For this study, 100 mg of glucose was dissolved in 14 ml of ethanol and then 100 mg of the solid catalyst candidate was suspended in this solution by sonication for 120 seconds. The suspension obtained was then constantly stirred in an oil bath at 80°C for an appropriate time (5–120 minutes). After the reaction, the solid was filtered off and the remaining solvent was

evaporated. The amounts of residual glucose and fructose dissolved in D_2O of 0.7 mL were quantified by ^{1}H-NMR spectroscopy using the internal standard method.[8] For this purpose, ethanol at a concentration of 10 mol% relative to the initial glucose concentration was used as the internal standard (Figure SE1). The concentrations of the sugars were determined by integration of the following regions: fructose (2H δ 4.10−3.98) and glucose (1H δ 3.20−3.26) relative to ethanol (3H δ 1.15–1.21) signals. To validate our quantification method, glucose-fructose mixtures with known concentrations were prepared and both the glucose and fructose concentrations were determined using the proposed method. The results obtained showed a good correlation with the real concentrations and had a standard error of ±5 % (Figure SE2). Fructose selectivity was defined as follows:

$$S(fructose) = \frac{\text{fructose yield mol\%}}{\text{glucose conversion mol\%}} \times 100\% \qquad \text{S3}$$

After the isomerization, the Mg_2Al-LDH catalyst was separated from the reaction mixture by centrifugation followed by thorough washing with ethanol and water. The catalyst samples were recycled in the following runs under the same reaction conditions as it was in the first run. To prove the heterogeneous nature of the reactions, the hot filtration test was performed. The catalyst (Mg_2Al-LDH) was filtrated from the reaction mixture before completion of the transformation (around 40% glucose conversion) and then the filtrate was further stirred under same reaction conditions as it was used before the filtration.
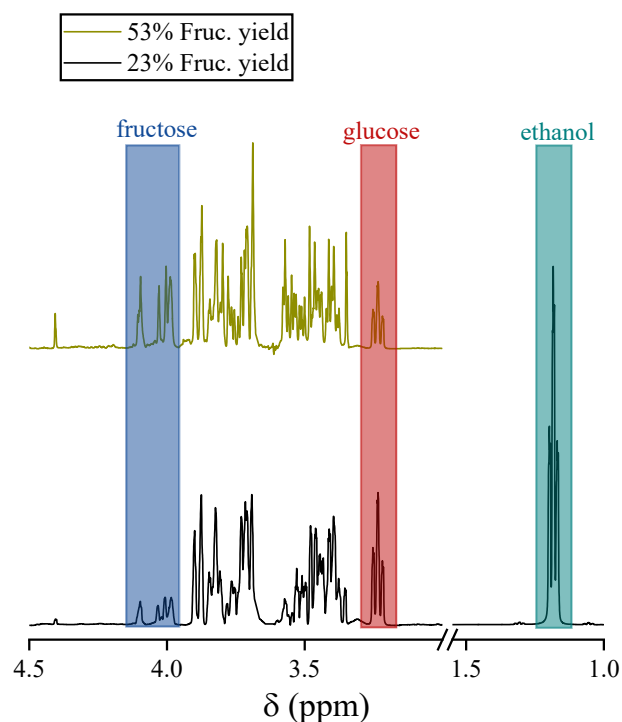
Fig. SE1 ^{1}H-NMR spectra of glucose-fructose mixture after LDH catalysed isomerization reaction of glucose. (Examples: Mg$_2$Al-LDH catalysed reaction (black), dehydrated (135°C) Mg$_4$Al-LDH catalysed reaction (tea-coloured)). Reaction conditions: glucose (100 mg), ethanol (14 mL), catalyst (100 mg), T = 80°C, t = 2h.
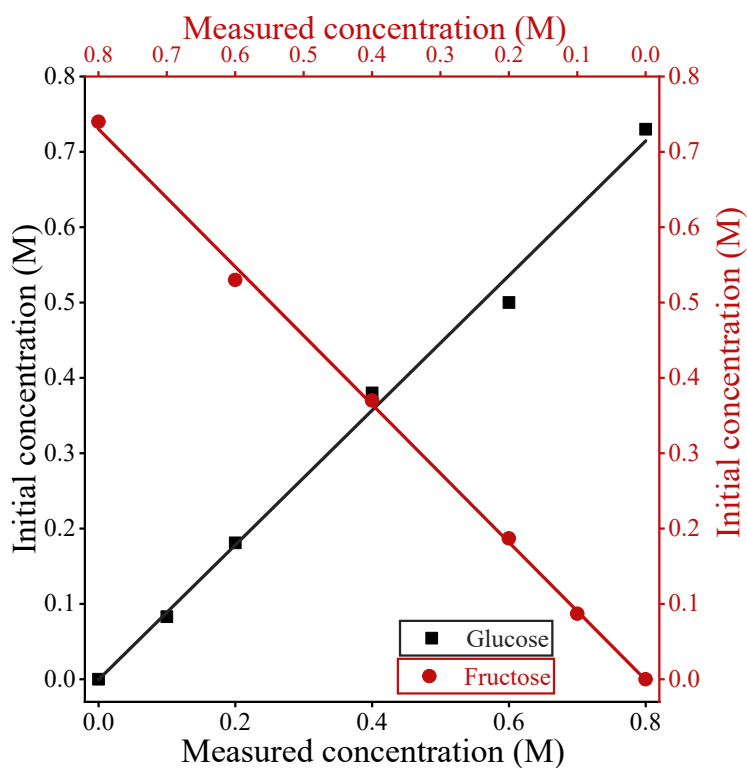
Fig. SE2 Comparative figure: initial concentrations of glucose/fructose in calibration solutions as a function of measured concentrations of fructose/glucose. ^{1}H-NMR spectroscopy method was used to determine the concentrations, using ethanol as internal standard (10 mol% relative to initial glucose concentration).

Section S2.

Supporting results and comparative data
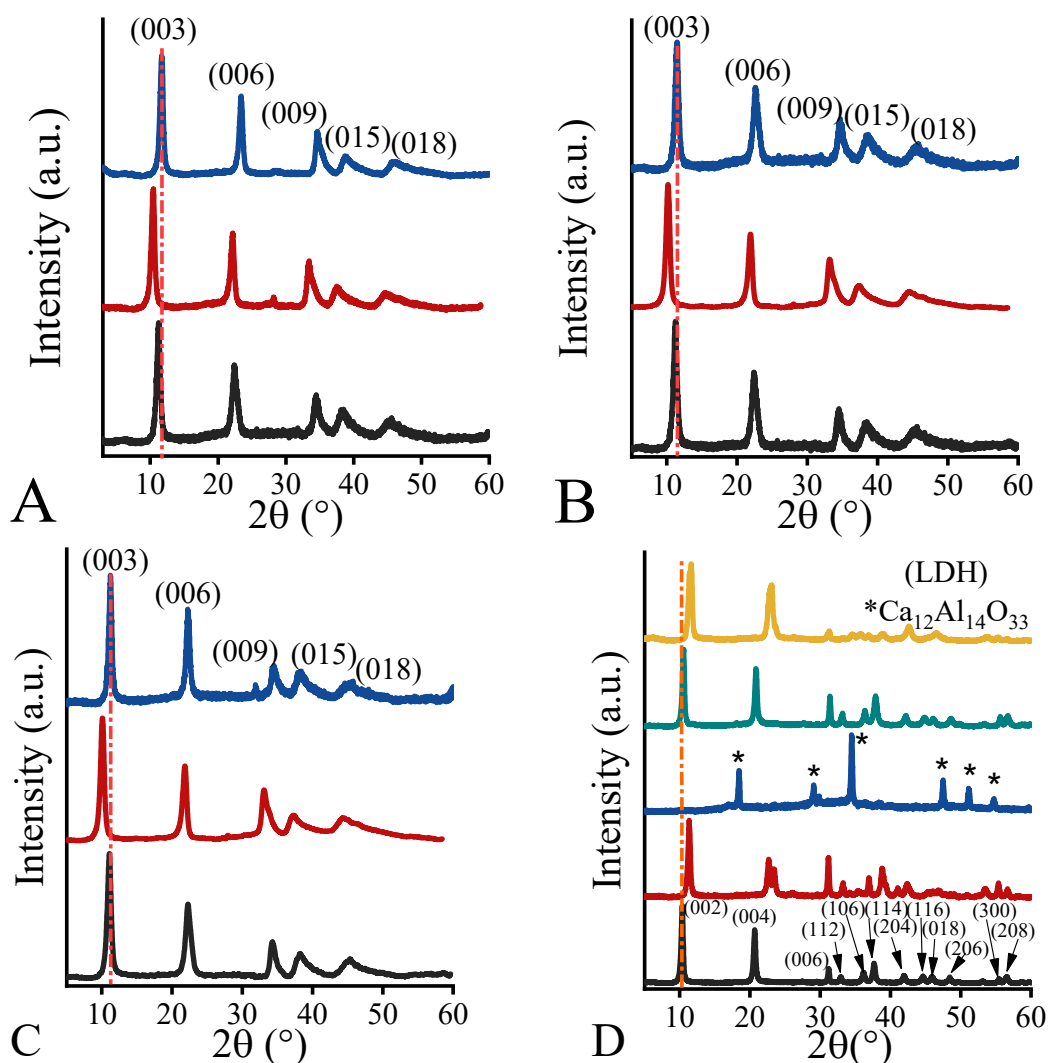
Fig. S1 XRD patters of the as-prepared CO_3–Mg_XAl-LDH (black), NO_3–Mg_XAl-LDH (wine-coloured), Cl–Mg_XAl-LDH (blue) counterparts of Mg_2Al-LDH (A), Mg_3Al-LDH (B) and Mg_4Al-LDH (C). XRD patterns of as-prepared NO_3-containing (black), as-prepared Cl-containing (wine-coloured), calcined (blue), NO_3-containing calcined-rehydrated (turquoise green) and CO_3-containing calcined-rehydrated (ochre) counterparts of Ca_2Al-LDH.
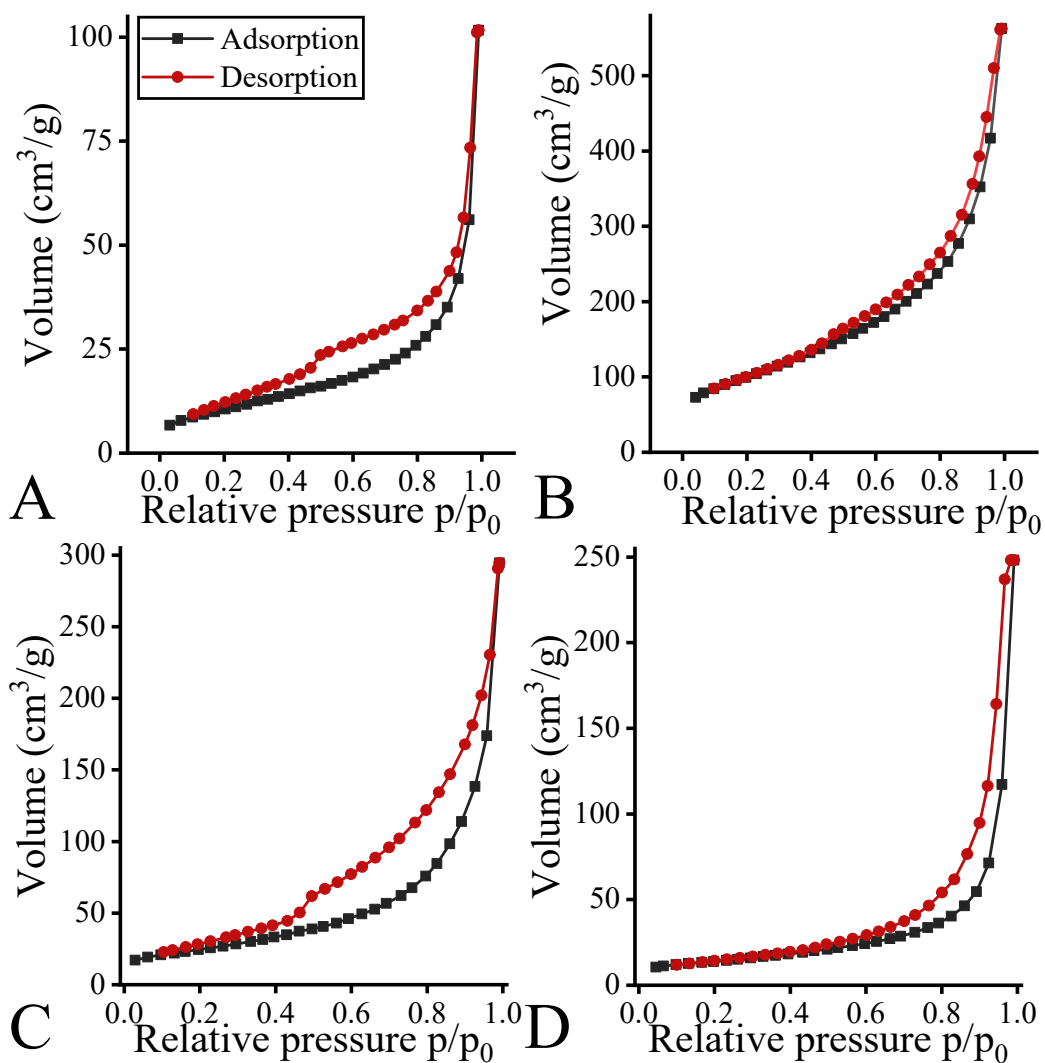
Fig. S2 Typical BET isotherms of as-prepared (A), calcined (B), calcined-rehydrated (C) and spent (D) layered double hydroxides. (These examples are related to Mg_2Al-LDH.)
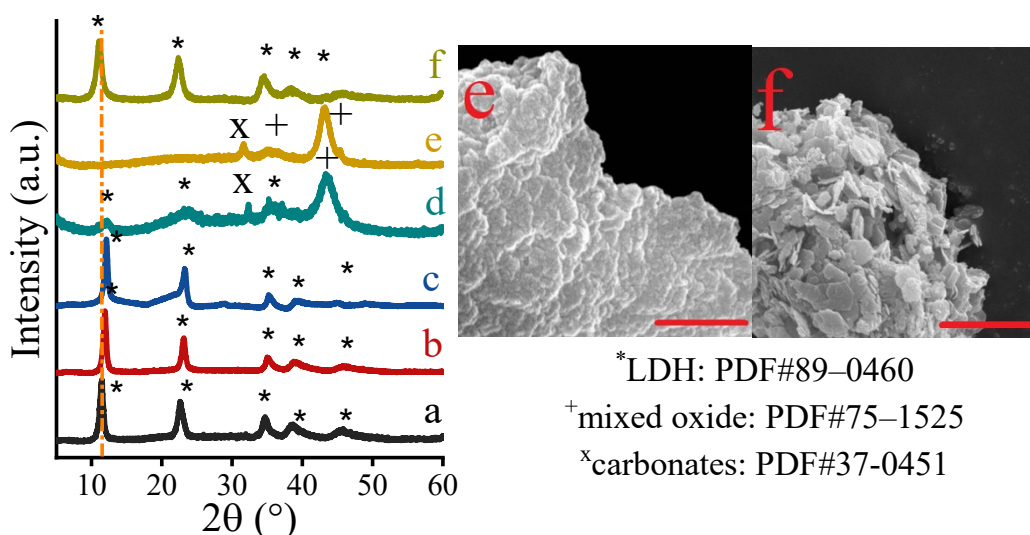
Fig. S3 XRD patterns of the heat-treated as well as rehydrated Mg$_3$Al-LDH: as-prepared (25°C) (a); dehydrated at 135°C (b); dehydrated at 200°C (c); dehydrated at 330°C (d); calcined at 500°C (e) as well as calcined-rehydrated (f). SEM micrographs of the calcined (e) and calcined-rehydrated (f) LDHs. JCPDS cards of the identified phases can be seen. Scale bars represent 500 nm.
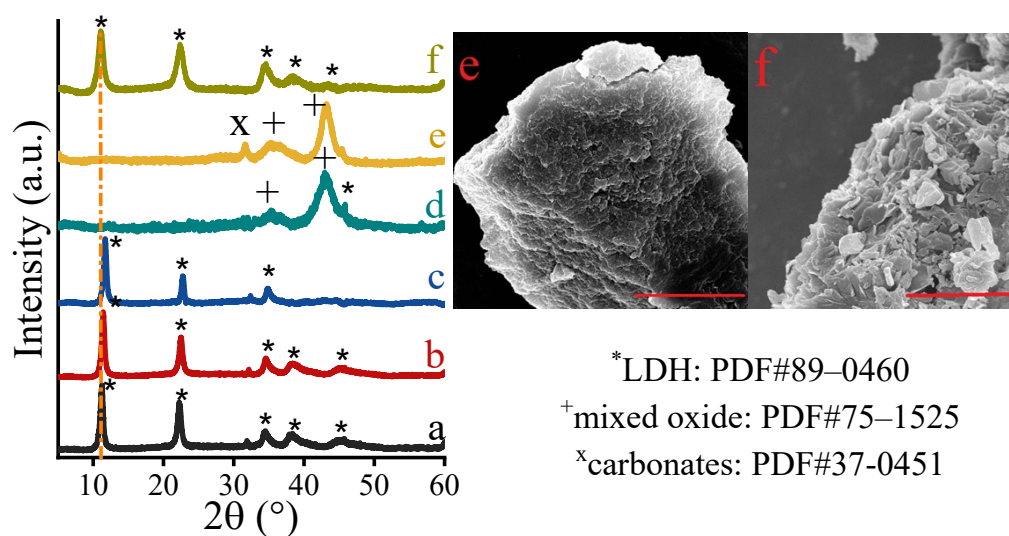
Fig. S4 XRD patterns of the heat-treated as well as rehydrated Mg$_4$Al-LDH: as-prepared (25°C) (a); dehydrated at 135°C (b); dehydrated at 200°C (c); dehydrated at 330°C (d); calcined at 500°C (e) as well as calcined-rehydrated (f). SEM micrographs of the calcined (e) and calcined-rehydrated (f) LDHs. JCPDS cards of the identified phases can be seen. Scale bars represent 500 nm.
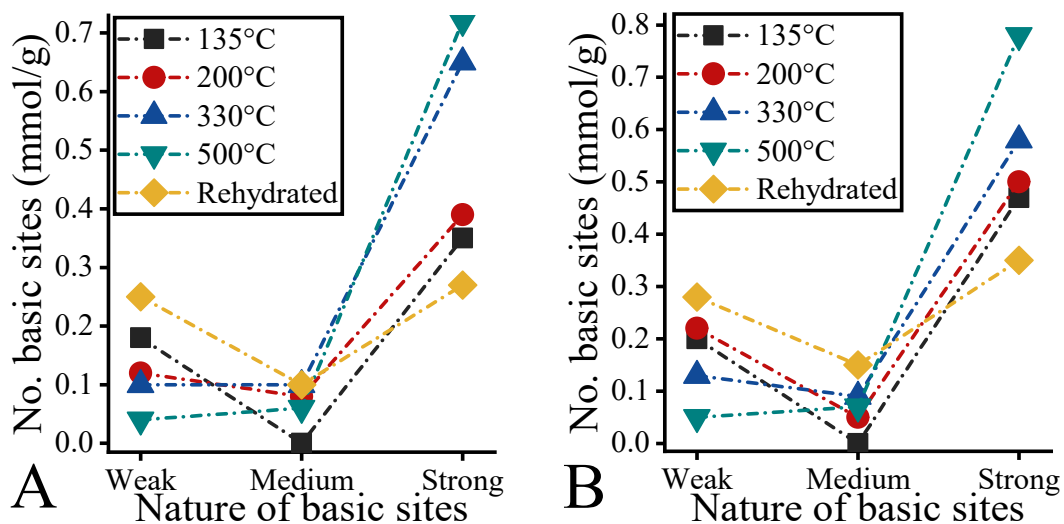
Fig. S5 Plot of the total number of basic sites for heat-treated and rehydrated Mg_3Al-LDH (A) and Mg_4Al-LDH (B).
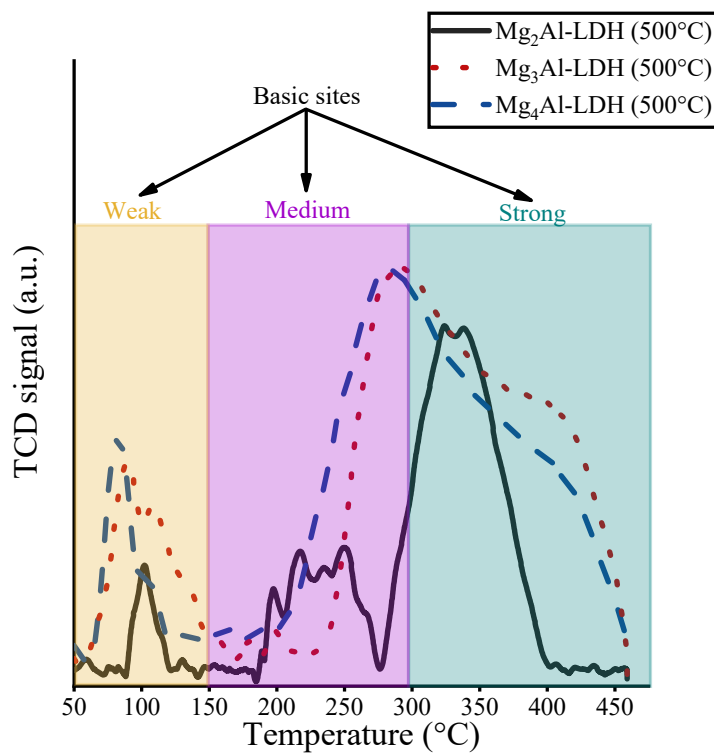
Fig. S6 CO_2-TPD profiles of the calcined (500°C) hydrotalcite structures.
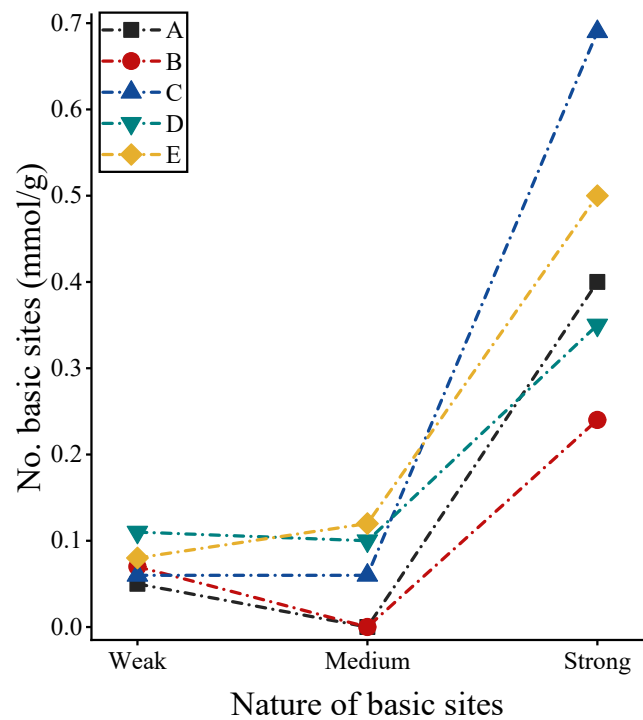
Fig. S7 Plot of the total number of basic sites for as-prepared NO_3-containing(A), as-prepared Cl-containing (B), calcined (C), NO_3-containing calcined-rehydrated (D) and CO_3-containing calcined-rehydrated (E) counterparts of hydrocalumite (Ca_2Al-LDH).
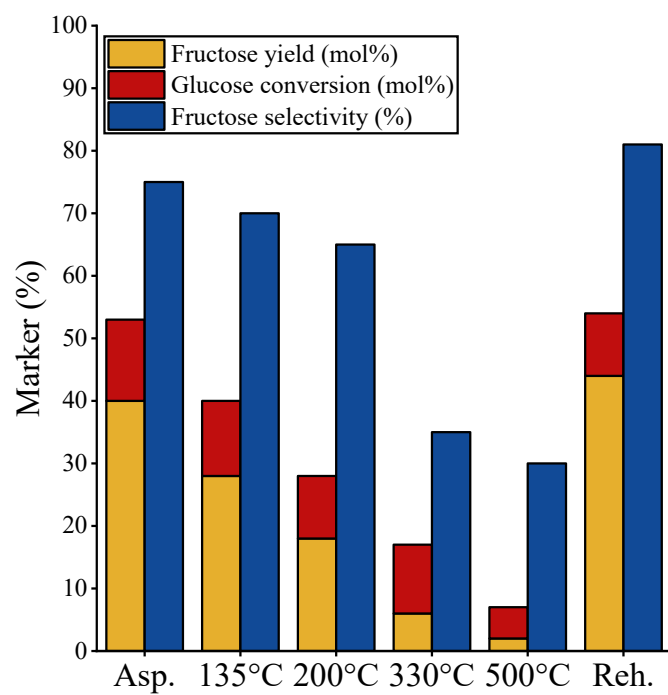
Fig. S8 Catalytic performances of the as-prepared and treated Mg₃Al-LDH. Reaction conditions: glucose (100 mg), ethanol (14 mL), catalyst (100 mg), T = 80°C, t = 2h.
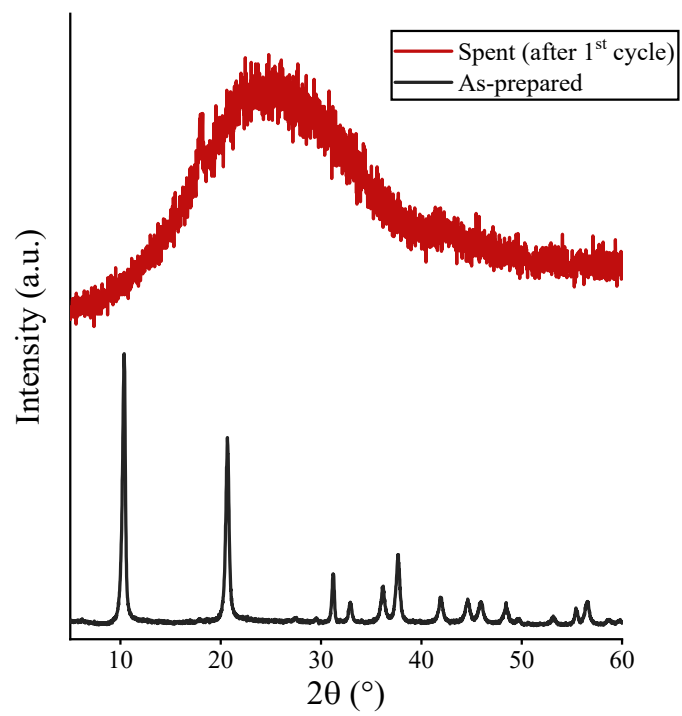
Fig. S9 XRD patterns of as-prepared and spent NO_3–Ca_2Al-LDH.

Table S1 Characteristics of the as-prepared hydrocalumites.

Hydrocalumite	Interlamellar distance (Å)[1]	Crystallite size (nm)[2]	Actual M(II):M(III) ratio[3]	Intrinsic basicity (mmol/g)[4]	Specific surface area (m²/g)[5]	Zeta potential (mV)[6]
As-prepared (nitrate)	8.6	35.1	2.01	0.45±0.03	15	+6
As-prepared (chloride)	7.9	38.4	2.00	0.31±0.01	11	+8
Calcined (500°C)	—	29.0	—	0.81±0.05	30	—
Rehydrated (nitrate)	8.5	34.8	1.97	0.56±0.02	17	+4
Rehydrated (carbonate)	7.6	19.2	1.96	0.70±0.06	55	-3

1: d(003), calculated by Bragg's law; 2: D(003), calculated by Scherrer equation; 3: determined by ICP-MS; 4: determined by non-aqueous acid-base titration; 5: determined by N_2 sorption (BET); 6: determined by DLS measurements.

Table S2 Characteristics of the heat-treated and rehydrated Mg_3Al-LDH.

Heat treatment (°C)	Interlamellar distance (Å)[1]	Crystallite size (nm)[2]	Actual M(II):M(III) ratio[3]	Intrinsic basicity (mmol/g)[4]	Specific surface area (m²/g)[5]
135	7.9	14.5	—	0.53	—
200	7.9	14.2	—	0.59	109
330	7.7	3.9 (6.0*)	—	0.85	191
500	—	7.2	2.99	0.82	360
500 (rehydrated)	8.1	13.9	2.94	0.62	185

1: d(003), calculated by Bragg's law; 2: D(003), calculated by Scherrer equation; 3: determined by ICP-MS; 4: determined by non-aqueous acid-base titration; 5: determined by N_2 sorption (BET). *Mixed oxide

Table S3 Characteristics of the heat-treated and rehydrated Mg_4Al-LDH.

Heat treatment (°C)	Interlamellar distance (Å)[1]	Crystallite size (nm)[2]	Actual M(II):M(III) ratio[3]	Intrinsic basicity (mmol/g)[4]	Specific surface area (m²/g)[5]
135	8.0	17.3	—	0.67	—
200	7.95	17.1	—	0.77	96
330	7.95	1.9 (5.5*)	—	0.80	154
500	—	7.4	3.99	0.80	315
500 (rehydrated)	8.1	15.8	3.95	0.78	161

1: d(003), calculated by Bragg's law; 2: D(003), calculated by Scherrer equation; 3: determined by ICP-MS; 4: determined by non-aqueous acid-base titration; 5: determined by N_2 sorption (BET). *Mixed oxide

Table S4 Characteristics of the as-prepared nitrate and chloride-containing hydrotalcites.

Hydrotalcite	Interlamellar anion	Interlamellar distance (Å)[1]	Crystallite size (nm)[2]	Intrinsic basicity (mmol/g)[3]
Mg$_2$Al-LDH	nitrate	8.5	16.00	0.27±0.01
	chloride	7.7	13.09	0.21±0.01
Mg$_3$Al-LDH	nitrate	8.8	16.10	0.37±0.03
	chloride	8.0	14.40	0.33±0.01
Mg$_4$Al-LDH	nitrate	8.9	16.92	0.49±0.04
	chloride	8.1	19.00	0.45±0.03

1: d(003), calculated by Bragg's law; 2: D(003), calculated by Scherrer equation; 3: determined by non-aqueous acid-base titration.

Table S5 Basicity quantitative evaluation of calcined (500°C) layered double hydroxides. CO$_2$-Temperature programmed Desorption results.

LDH*	Weak basic sites (mmol/g)	Medium-Strong basic sites (mmol/g)	Total amount of basic sites (mmol/g)
Mg$_2$Al	0.23	1.48	1.71
Mg$_3$Al	0.43	1.66	2.09
Mg$_4$Al	0.37	1.92	2.29

*calcined at 500°C

Table S6 BET surface area of as-prepared, alcohol-treated and "glucose-treated" hydrotalcites.

Specific surface area (m^2/g)	Mg$_2$Al-LDH	Mg$_3$Al-LDH	Mg$_4$Al-LDH
As-prepared	71	64	56
Alcohol-treated	115	110	101
Stirred with glucose	59	88	100

Table S7 Comparative table of the catalytic ability of the as-prepared NO_3–Mg_2Al-LDH catalyst and the benchmark catalysts for glucose-to-fructose isomerization.

Catalyst	Glucose conversion (%)	Fructose selectivity	Solvent	Reaction temperature (°C)	Reference
NO$_3$–Mg$_2$Al-LDH	71	83	Ethanol	80	**This work**
Hydrotalcite	65	80	Ethanol	120	3
	62	82	1-Butanol	120	9
	30	87	Water	110	7
	27	75	Water	120	10
	50	70	Water	90	11
	58	73	Water	90	12
	42	88	Water	100	13
	65	50	Water	130	14
	42	90	N,N-dimethylformamide	100	15
	59	33	Water	120	16
Lysine	38	80	Water	120	17
Triethylamine	54	57	Water	100	18
H-USY	63	42	Water	120	19
Al$_2$O$_3$	60	46	Water	120	20
N-doped Biochar	24	80	Acetone/Water	160	20

Italic: heterogeneous catalysts

REFERENCES

1   G. Varga, Z. Somosi, Z. Kónya, Á. Kukovecz, I. Pálinkó and I. Szilagyi, *J. Colloid Interface Sci.*, 2021, **581**, 928–938.

2   I. Pálinkó, P. Sipos, O. Berkesi and G. Varga, *J. Phys. Chem. C*, 2022, **126**, 15254–15262.

3   M. Yabushita, N. Shibayama, K. Nakajima and A. Fukuoka, *ACS Catal.*, 2019, **9**, 2101–2109.

4   Z. P. Xu, G. Stevenson, C. Q. Lu and G. Q. Lu, *J. Phys. Chem. B*, 2006, **110**, 16923–16929.

5   Y. Zhao, F. Li, R. Zhang, D. G. Evans and X. Duan, *Chem. Mater.*, 2002, **14**, 4286–4291.

6   D. W. J. Leung, C. Chen, J. C. Buffet and D. O'Hare, *Dalton Trans.*, 2020, **49**, 9306–9311.

7   I. Delidovich and R. Palkovits, *J. Catal.*, 2015, **327**, 1–9.

8   J. M. Carraher, C. N. Fleitman and J. P. Tessonnier, *ACS Catal.*, 2015, **5**, 3162–3173.

9   P. P. Upare, A. Chamas, J. H. Lee, J. C. Kim, S. K. Kwak, Y. K. Hwang and D. W. Hwang, *ACS Catal.*, 2020, **10**, 1388–1396.

10 I. K. M. Yu, A. Hanif, D. C. W. Tsang, J. Shang, Z. Su, H. Song, Y. S. Ok and C. S. Poon, *Chem. Eng. J.*, 2020, **383**, 122914.

11 S. Yu, E. Kim, S. Park, I. K. Song and J. C. Jung, *Catal. Commun.*, 2012, **29**, 63–67.

12 I. Delidovich and R. Palkovits, *Catal. Sci. Technol.*, 2014, **4**, 4322–4329.

13 G. Lee, Y. Jeong, A. Takagaki and J. C. Jung, *J. Mol. Catal. A Chem.*, 2014, **393**, 289–295.

14 S. Park, D. Kwon, J. Y. Kang and J. C. Jung, *Green Energy Environ.*, 2019, **4**, 287–292.

15 D. Kwon, J. Y. Kang, S. An, I. Yang and J. C. Jung, *J. Energy Chem.*, 2020, **46**, 229–236.

16 X. Ye, X. Shi, J. Li, B. Jin, J. Cheng, Z. Ren, H. Zhong, L. Chen, X. Liu, F. Jin and T. Wang, *Chem. Eng. J.*, 2022, **440**, 135844.

17 Q. Yang, M. Sherbahn and T. Runge, *ACS Sustain. Chem. Eng.*, 2016, **4**, 3526–3534.

18 C. Liu, J. M. Carraher, J. L. Swedberg, C. R. Herndon, C. N. Fleitman and J. P. Tessonnier, *ACS Catal.*, 2014, **4**, 4295–4298.

19 S. Saravanamurugan, M. Paniagua, J. A. Melero and A. Riisager, *J. Am. Chem. Soc.*, 2013, **135**, 5246–5249.

20 D. M. Gao, Y. B. Shen, B. Zhao, Q. Liu, K. Nakanishi, J. Chen, K. Kanamori, H. Wu, Z. He, M. Zeng and H. Liu, *ACS Sustain. Chem. Eng.*, 2019, **7**, 8512–8521.